

EXTREME DRAG FORCES AND THE SURVIVAL OF WIND- AND WATER-SWEPT ORGANISMS

MARK W. DENNY

*Department of Biological Sciences, Stanford University, Hopkins Marine Station,
Pacific Grove, CA 93950, USA*

Accepted 17 May 1994

Summary

A stationary organism exposed to steady turbulent flow is subjected to a drag force that fluctuates about a mean, and when the drag on the organism is characterized, it is traditionally this mean force that is cited. Important information is lost, however, when the fluctuations in drag are ignored. This is particularly true when extreme drag forces are relevant; for instance, when predicting the survival of benthic animals on wave-swept shores and in torrential streams, or of plants in windblown terrestrial habitats.

This study reports on the probability distribution of drag fluctuations for five objects: a flat plate, large and small cylinders, a sphere and a limpet shell. Distributions vary substantially among different objects exposed to the same mainstream flow; the sphere and limpet exhibit larger fluctuations than the plate and cylinders. The distribution of extremes in drag is used to predict the likelihood that an organism will be dislodged. For organisms in which the applied fluid-dynamic stress is near the mean breaking stress (e.g. some corals, trees and mussels), calculations made using the extreme drag can yield a probability of dislodgment substantially higher than that calculated using the average.

Introduction

Water velocities in mountain streams and rain-swollen rivers may reach 9 m s^{-1} , and the concomitant hydrodynamic forces can have important effects on the feeding, habitat selection and survival of fluvial benthic organisms (Hynes, 1970; Vogel, 1981). Winds may exceed 45 m s^{-1} in severe storms, and the resulting drag forces can topple trees (Oliver and Mayhead, 1974; Grace, 1977; Vogel, 1981). Similarly, ocean waves are accompanied by water velocities as high as 14 m s^{-1} and can impose substantial hydrodynamic forces on intertidal and shallow subtidal marine plants and animals (e.g. Koehl, 1984; Denny *et al.* 1985; Denny, 1988). The largest of these forces may play a role in determining individual survivorship, species distributions, patch dynamics and the evolution of body size and form on wave-swept shores (for reviews, see Koehl, 1984; Seymour *et al.* 1989; Denny *et al.* 1985; Denny, 1988, 1993, 1994).

Recently, attempts have been made to predict maximal wave-induced forces by coupling the theory of wave height distributions with empirical information regarding

Key words: drag, turbulence, disturbance, survivorship, biomechanics, fluid-dynamics, limpet.

flow in breaking waves (Denny and Gaines, 1990; Denny, 1991, 1993, 1994). Application of this method to the prediction of the 'birth rate' of bare patches of substratum in mussel beds results in values that are in approximate agreement with the range found in nature (Denny, 1993, 1994). This preliminary success bodes well for the use of fluid-dynamic principles as predictive tools in the study of ecology.

The ultimate utility of this approach depends, however, on the accuracy with which the stress exerted on an individual can be predicted from a knowledge of fluid velocity. Therein lie potential difficulties.

Consider drag, a fluid-dynamic force that acts to push an object downstream. For the high fluid velocities encountered in surf zones, terrestrial storms and mountain streams, drag is traditionally described by the equation:

$$\text{Drag} = \frac{1}{2}\rho u_{\infty}^2 A_p C_D, \quad (1)$$

where ρ is the density of the fluid (approximately 1000 kg m^{-3} for fresh water, 1025 kg m^{-3} for sea water and 1.2 kg m^{-3} for air), u_{∞} is mainstream velocity relative to the organism (measured just outside the local boundary layer surrounding the organism and averaged over a suitable period) and A_p (the profile area) is the area of the organism projected onto a plane perpendicular to the direction of mainstream fluid motion. C_D is the *drag coefficient*, an index of the effect the organism's shape has on the pattern of flow.

In this report, I address a potential complication in the application of equation 1. Flow in mountain streams, breaking waves and storm winds is characterized by intense turbulence. That is, in addition to the relatively orderly flow of air or water past an organism associated with the bulk motion of the fluid, there is a rapid fluctuation in velocity associated with the convection of turbulent eddies (Tennekes and Lumley, 1972). Although it is reasonable to suppose that turbulent fluctuations in velocity can affect the drag imposed on a stationary organism in otherwise steady flow, these effects have not been fully explored.

The standard technique for measuring time-averaged drag in turbulent flow is as follows. The organism in question (or a model of it) is attached to a force transducer and placed in flow of known average mainstream velocity. The resulting voltage output from the transducer (which is proportional to the force) fluctuates about some mean value as the transducer responds to the drag imposed by the instantaneous flow around the organism. The mean voltage is viewed as the drag signal, and the fluctuations in voltage are viewed as 'noise'. It is convenient to rid the voltage signal of this noise by mechanically damping the transducer using a dashpot or by passing the voltage signal through a low-pass filter (either electronic or numerical) with a cut-off frequency well below the dominant frequency of the noise. A clean measure of the time-averaged force corresponding to a given mean velocity is thereby obtained.

Unfortunately, the mean drag may not be the most biologically relevant value in a surf zone, mountain stream or gale. Rather, it is the *maximal* drag that is likely to be of importance in determining whether an organism will be broken or dislodged. By low-pass filtering the output from a transducer, information regarding the maximal drag force is lost.

I report here on measurements of extreme drag forces in unidirectional turbulent flow,

the relationship between these extreme values and their corresponding means, and the potential biological consequences of these results.

Materials and methods

Drag was measured on five objects: an acrylic plastic sphere (2.17 cm in diameter), two acrylic plastic cylinders (one 1.11 cm in diameter, 4.04 cm high; the other 0.63 cm in diameter, 2.25 cm high), a thin aluminum plate oriented broadside to flow (0.89 cm wide, 3.03 cm high, 0.16 cm thick) and a limpet shell (*Lottia pelta* Rathke, 1.43 cm high, 3.03 cm long, 2.50 cm wide) oriented broadside to flow with its right side upstream. The nonbiological objects were lightly sanded with 400 grit paper to provide a uniform surface texture.

Drag measurements were conducted in a unidirectional flow tank with a working section 10 cm square (Denny, 1988; Carrington, 1990). During the measurement of drag fluctuations, the mean mainstream velocity was 3.04 m s^{-1} , measured using a Pitot tube outside the boundary layer and a static port in the wall of the tank's working section. In an additional set of experiments, u_∞ was varied from 2.0 to 3.5 m s^{-1} to allow C_D to be measured as a function of velocity.

To characterize the boundary layer at a mainstream velocity of 3.04 m s^{-1} , the velocity near the wall was measured (again using the Pitot tube, diameter 1.1 mm) at increments from the wall of approximately 0.6 mm. In a typical turbulent boundary layer over a smooth wall (such as that found in these tests), the time-averaged velocity at a distance z from the wall is (for the inner 20% of the boundary layer):

$$u(z) = (u^*/k)\ln(z/z_0), \quad (2)$$

where u^* is the friction velocity, k is von Kármán's constant ($k=0.41$) and z_0 is the roughness height (Schlichting, 1979; Middleton and Southard, 1984). Thus, the slope of a plot of time-averaged velocity as a function of the natural logarithm of distance from the wall equals u^*/k , from which u^* itself can be calculated. The friction velocity is defined to be:

$$u^* \equiv \langle u'w' \rangle^{1/2}, \quad (3)$$

where u' is the deviation from the mean of the velocity parallel to the wall (the velocity fluctuation of interest here) and w' is the deviation from the mean of the velocity perpendicular to the wall (Schlichting, 1979; Middleton and Southard, 1984). The angular brackets ($\langle \rangle$) denote that the temporal average is taken of the product $u'w'$; thus, u^* depends both on the magnitudes of u' and w' and on their correlation. The degree of correlation between u' and w' can be expressed as the coefficient of correlation Φ :

$$\Phi = \frac{\langle u'w' \rangle}{\sqrt{\langle u'^2 \rangle} \sqrt{\langle w'^2 \rangle}}. \quad (4)$$

In turbulent boundary layers, the maximal correlation coefficient for u' and w' is about 0.4 and $\sqrt{\langle w'^2 \rangle} \approx u^*$ (Schlichting, 1979). As a result, the average deviation in velocity near the wall, u'_{rms} ($=\sqrt{\langle u'^2 \rangle}$), is approximately $2.5u^*$, and the measurement of u^* thus

provides a method of estimating the magnitude of turbulent fluctuations in velocity in the direction of flow. For a verification of this effect under field conditions, see Williams *et al.* (1989).

Drag was measured using the transducer described by Carrington (1990). The object to be tested was attached to a circular plate held flush with the ceiling of the working section by parallel stainless-steel beams. Any force applied to the plate along the direction of flow resulted in a deflection of the beams, the deformation of strain gauges glued to the beams and, ultimately, a voltage signal. The resonant frequency of the transducer was approximately 59 Hz, and the beams were underdamped. To avoid complications from resonant vibrations of the transducer, its voltage signal was electronically low-pass-filtered to approximate that of a slightly overdamped beam. With this simple RC filter in place, the transducer responded to the instantaneous release of a statically applied force with a rapid decay in its voltage signal and no overshoot past the zero-force voltage. The time constant of this response was approximately 0.024 s.

The transducer's response time can be compared with the period of velocity fluctuations expected for flow in the vicinity of the test objects. Ideally, these fluctuations would be measured directly, using a hot-wire anemometer or a laser Doppler velocity meter. Lacking these tools, I instead estimated the period of fluctuation in two, indirect ways.

First, the size of the most energetic eddies in boundary-layer turbulence is approximately equal to the distance from the substratum at which the velocity fluctuations are measured (Schlichting, 1979; Tennekes and Lumley, 1972). For the objects used in these experiments (height 1.4–4 cm), the relevant length scale for the turbulence is thus 1.4–4 cm. One would expect that the spectrum of velocity fluctuations would have a broad peak at a period equal to this length scale divided by the average mainstream velocity (3.04 m s^{-1}); that is, a period of approximately 0.003–0.013 s.

Alternatively, objects in flow could respond primarily to the velocities caused by turbulent 'sweeps' as energetic eddies are convected near to the wall. The interval T between sweeps may be as short as:

$$T = 2.5\delta/u_{\infty}, \quad (5)$$

where u_{∞} is the time-averaged mainstream velocity and δ is the boundary-layer thickness (Cantwell, 1981). In these experiments, $\delta \approx 1.2 \text{ cm}$ (see Results), suggesting that the interval between sweeps may be as little as 0.01 s.

Both of these approaches suggest that the maximal fluctuations in water velocity are likely to be applied for a period shorter than the response time of the transducer (0.024 s) and therefore suggest that the transducer may underestimate the maximal drag experienced by rigid biological objects. It should be noted, however, that many biological objects are not rigid. The shell of a snail or limpet is supported on a muscular foot that results in some compliance in the presence of flow. The bodies of insects that inhabit torrential streams are similarly held in place by compliant appendages. Trees, grasses, gorgonians, anemones and many macroalgae are more compliant still. Thus, though the transducer used in these experiments may underestimate the maximal drag that would be experienced by a rigid organism, it may also overestimate the maximal drag felt by flexible organisms. In this respect, the transducer used here was chosen as a

practical compromise. The potential consequences of its response time will be discussed below.

The transducer was calibrated prior to each experiment using standard weights, and a measure of the temporal running average of drag was obtained by filtering the transducer output using a separate low-pass RC filter with a time constant of approximately 1 s. All drag measurements were corrected for the small amount of friction drag acting on the exposed area of the mounting plate.

The drag imposed on each test object was recorded for 1000 s on a Gould model 220 two-channel oscillographic chart recorder. This recorder is capable of accurately recording full-scale deflections with frequencies up to 60 Hz, well in excess of the frequencies produced by the force transducer. The simultaneous drag records (both ‘noisy’ and averaged) were subsequently divided into 50 contiguous 20 s intervals, and the maximal force, F_{\max} , encountered in each interval was noted for the ‘noisy’ signal. For each interval, the maximal force was then expressed as a fractional deviation from the simultaneously recorded averaged force (F_{avg}). This normalized deviation (F_n) is:

$$F_n = (F_{\max}/F_{\text{avg}}) - 1. \quad (6)$$

The cumulative probability distribution of normalized deviations was then estimated. Values for F_n were ranked in ascending order, the smallest having the rank 1. The probability, $P(F_n)$, that the extreme drag in a randomly chosen interval is less than F_n is given by:

$$P(F_{n_i}) \approx i/(N + 1), \quad (7)$$

where N is the total number of intervals examined (in this case, 50) and i is the rank of the force (Gumbel, 1958). Ties between or among separate measurements of F_n are assigned an average rank. The cumulative probability distribution to which this empirical curve asymptotes was then estimated using a three-parameter model suggested by Jacocks and Kneile (1975):

$$P(F_n) = \exp - \{ [(\alpha - \beta F_n)/(\alpha - \beta \epsilon)]^{1/\beta} \}, \quad (8)$$

where $P(F_n)$ is the probability that the extreme normalized deviation in drag in a randomly chosen interval is less than F_n . α determines how fast $P(F_n)$ rises with the logarithm of time and ϵ is the modal (that is, the most probable) value of F_n . The coefficients in this equation were determined using a maximum likelihood criterion and an iterative, nonlinear curve-fitting routine (see Gaines and Denny, 1993, for details). This model is extremely flexible in its ability to fit cumulative probability curves (see Jacocks and Kneile, 1975; Sarpkaya and Isaacson, 1981). When α and β are both positive, the model takes one form of an extremal (or Gumbel) type III distribution, known as the Weibull upper bound distribution. When β is negative, the model has the general form of an extremal type II distribution (also known as a Fisher-Tippet, Cauchy, Fretchet type II or Gumbel type II distribution), with the precise form depending on the sign of α . If β approaches zero, the model asymptotes to an extremal (or Gumbel) type I distribution.

Note that if α and β are both positive and $F_n = \alpha/\beta$, then $P(F_n) = 1$. In this case, if the model of equation 8 holds, it is absolutely certain that the extreme force in a randomly chosen interval is less than F_n . Thus, when α and β are both positive, their ratio provides

an estimate of the expected absolute maximal normalized deviation in drag. If β is negative, a well-defined maximal Fn is not predicted by this analysis.

From the cumulative probability curve for Fn , the likelihood of encountering a given normalized extreme force can be calculated as a function of the time for which the object is exposed to flow. The expected time an organism must wait between occurrences of a given extreme (the *return time*, Tr ; Gumbel, 1958) is:

$$Tr = t_i / [1 - P(Fn)], \quad (9)$$

where t_i is the length of the interval used in the analysis (here, $t_i=20$ s).

Conversely, if the time for which the organism is exposed to flow (that is, the maximal return time Tr_{\max}) is known, the expected extreme Fn can be predicted from equation 9 and the inverse of equation 8:

$$Fn = (\alpha/\beta) - \{[(\alpha/\beta) - \epsilon] \{-\ln[1 - (t_i/Tr_{\max})]\}\}^\beta. \quad (10)$$

At any particular velocity, the likelihood of encountering a given extreme Fn increases with time.

Results

Turbulence and boundary-layer characteristics

Flow in the working section was substantially turbulent as shown by the velocity gradient adjacent to the substratum (Fig. 1A), which has a shape typical of turbulent boundary layers. When this boundary-layer profile is replotted (Fig. 1B), it closely approximates the logarithmic profile expected for the near-substratum portion of a well-developed turbulent boundary layer. The friction velocity estimated from the profile shown in Fig. 1B is approximately 0.199 m s^{-1} , 6.6 % of the mainstream velocity.

The boundary layer thickness (δ), defined as the distance from the substratum to the height at which $u(z)=0.99u_\infty$, was approximately 1.2 cm.

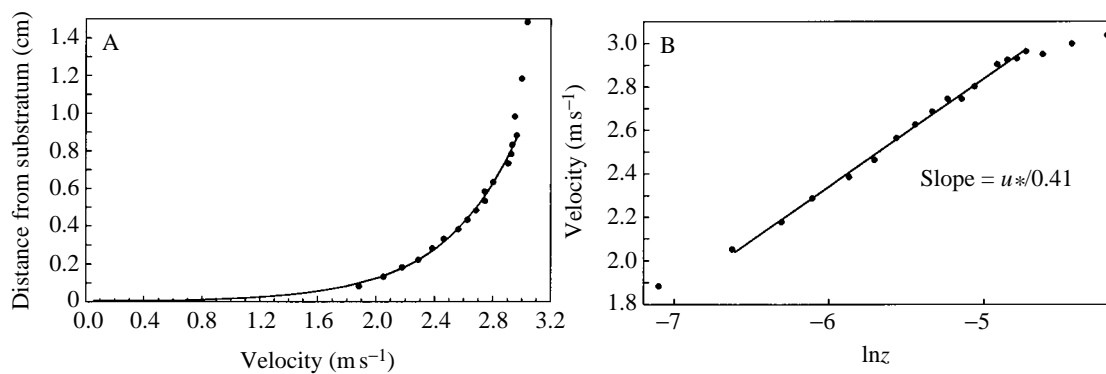


Fig. 1. The boundary-layer profile characteristic of these experiments. (A) The profile itself. The solid curve is a logarithmic fit to the 16 data points taken closest to the wall. (B) The data from A logarithmically transformed. The slope of the solid regression line is equal to the friction velocity (u^*) divided by von Kármán's constant, 0.41.

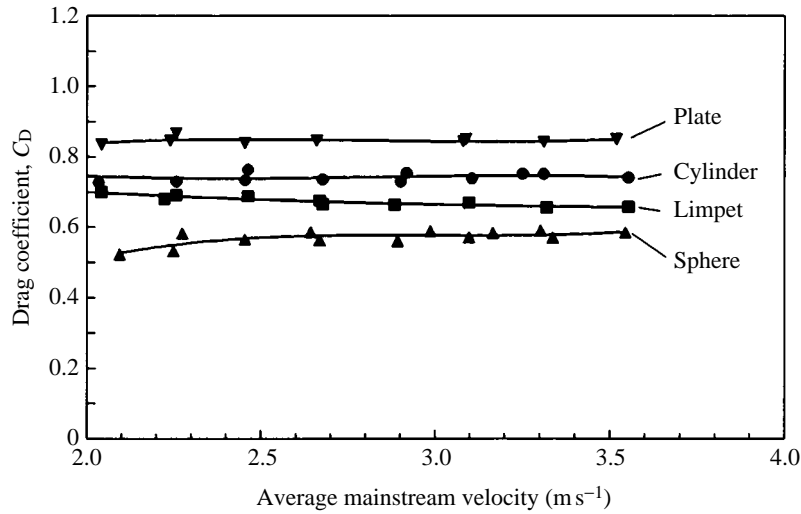


Fig. 2. Drag coefficient as a function of velocity for the objects used in this study. Within a wide range of average mainstream velocities, there is no significant variation in drag coefficient. Solid lines are third-order polynomial regressions for the entire data set for each object.

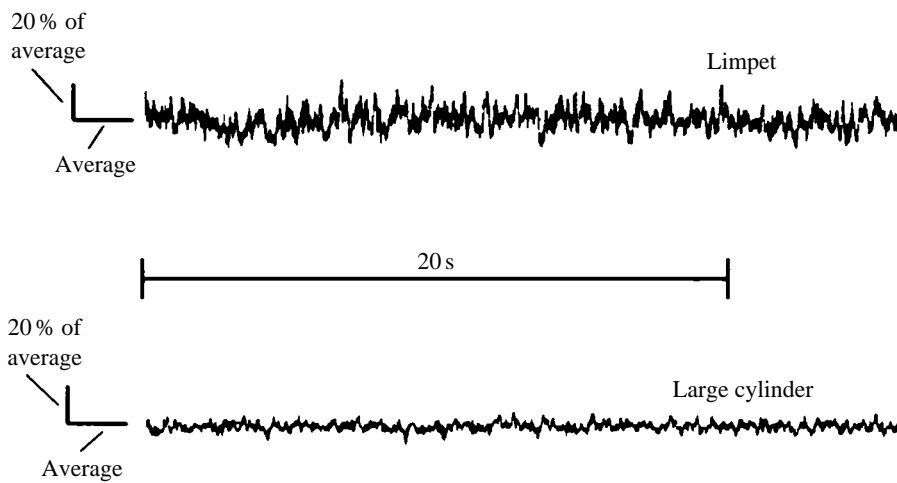


Fig. 3. Representative recordings of drag for the objects with the smallest variation (the large cylinder) and the largest variation (the limpet). The vertical scale shows 20% of the average drag recorded for the two objects, and the horizontal line marked 'average' is drawn at the level of the average force.

Drag measurements

The drag coefficients for the test objects (Fig. 2) vary negligibly across a wide range of velocities.

At a mainstream velocity of 3.04 m s^{-1} , all objects showed measurable deviations in

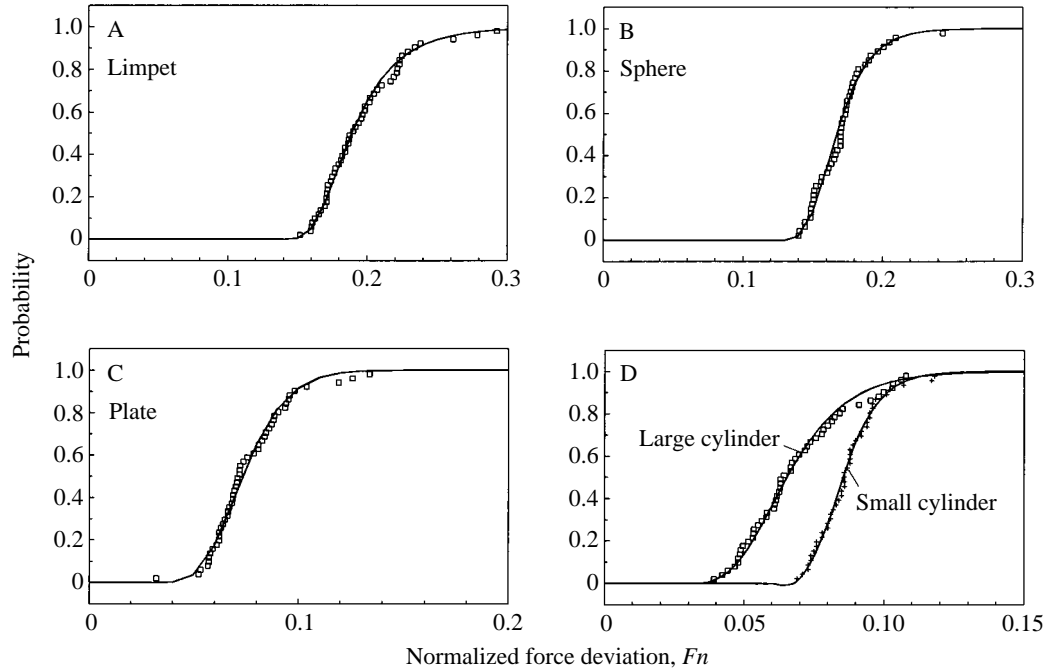


Fig. 4. Cumulative probability curves for the extreme drag forces measured on the experimental objects. Solid lines are estimates of the asymptotic probability distributions (calculated using equation 8). Note that the scale of the abscissa varies among plots.

Table 1. Coefficient values from the maximum likelihood estimates for a model of the probability distribution of maximal and minimal drag forces (see equation 8)

Object	α	ASE	β	ASE	ϵ	ASE	Absolute maximum F_n	S.E.M.
Large cylinder	0.016	0.012	0.018	0.183	0.060	0.003	0.860	0.590
Plate	0.023	0.008	0.099	0.103	0.068	0.004	0.234	0.154
Small cylinder	0.012	0.013	0.041	0.147	0.082	0.002	0.301	0.790
Sphere	0.017	0.028	0.005	0.166	0.161	0.004	3.160	0.731
Limpet	0.001	0.033	-0.110	0.180	0.182	0.005	Undefined	-

Standard errors for α , β and ϵ are renormalized asymptotic standard errors (ASE).

The standard errors for the ratio α/β (an estimate of the absolute maximum F_n) were calculated using a bootstrap algorithm (Efron and Tibshirani, 1993).

$F_{n_{\max}}$, the absolute maximum F_n , could not be defined for the limpet because of the negative value of β ; see text for further explanation.

drag force from the mean (for examples, see Fig. 3), and the extent of these deviations varied among objects (Fig. 4; Table 1). For instance, the most likely (modal) maximal

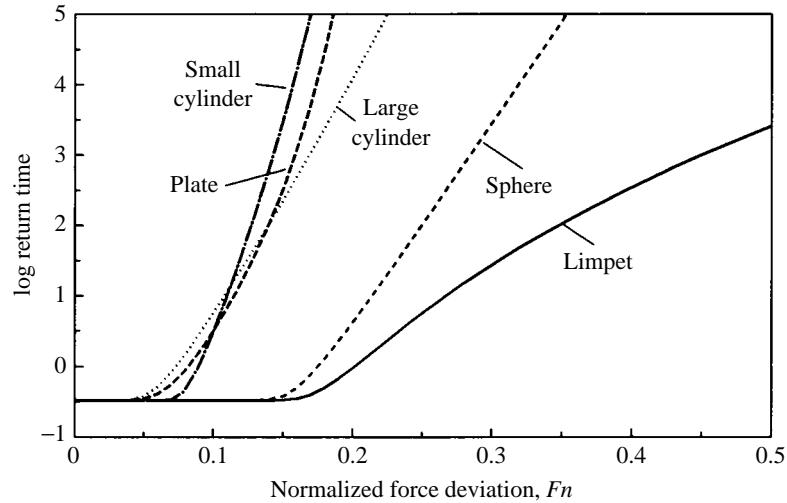


Fig. 5. Expected return times (min) calculated as a function of deviation from the mean drag.

drag exceeded the mean by only 6–8% in the cylinders and the flat plate ($\epsilon=0.060$ for the large cylinder, 0.068 for the flat plate, 0.082 for the small cylinder). In contrast, the modal maximal drag on the sphere exceeded the mean by approximately 16% ($\epsilon=0.161$) and the modal maximal drag on the limpet shell exceeded the mean by over 18% ($\epsilon=0.182$). Estimates of return times for Fn are shown in Fig. 5.

It is expected that the absolute maximal drag experienced by a flat plate is 23% greater than the mean ($\alpha/\beta=0.234$, Table 1), while that of a cylinder is 30–86% greater than the mean (depending on the size of the cylinder). In contrast, the expected absolute maximal drag experienced by a sphere is much larger, 316% of the mean. There is no well-defined limit to the maximal drag that may be experienced by a limpet (β is negative).

Discussion

Cause of drag fluctuations

The experiments performed here clearly demonstrate that drag can vary substantially for stationary objects in turbulent flow and that the magnitude of this fluctuation varies among objects. The experiments were not designed to elucidate the causes of drag fluctuation. Nonetheless, inferences can be drawn from the data.

There are three mechanisms that could conceivably contribute to the observed fluctuations in drag. (1) Turbulent fluctuations in ambient velocity result in fluctuations in the dynamic pressure imposed on the object and, thereby, in fluctuations in drag. (2) As eddies are shed from the object, fluctuations in the object's wake result in a variation in the upstream–downstream pressure difference across the object and, thereby, in a variation in drag. (3) A drastic variation in drag coefficient occurring over the range of velocities associated with the convection of turbulent eddies could result in substantial variation in drag. For instance, if the boundary layer of the object were near the transition

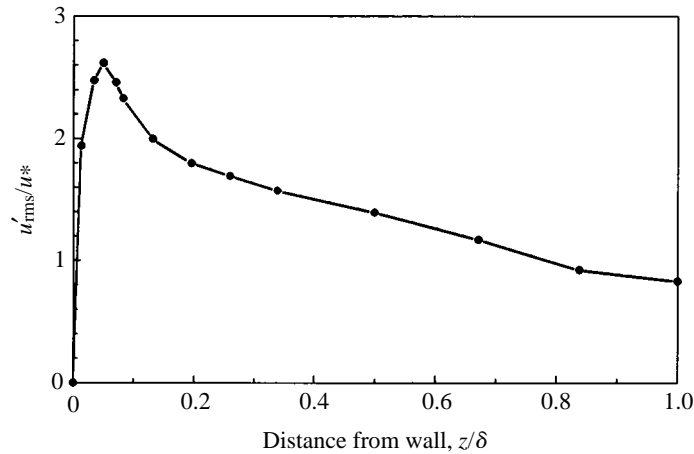


Fig. 6. The average fluctuation in velocity parallel to the wall (u'_{rms}) is a function of distance from the wall. Data calculated from information presented in Figs 18.3 and 18.4 in Schlichting (1979), taken in turn from Reichardt (1938).

from laminar to turbulent, a small fluctuation in ambient velocity would result in a large fluctuation in drag (see Vogel, 1981).

This last mechanism can be discounted because C_D varies negligibly across a wide range of velocities centered on the mainstream velocity used in these experiments (Fig. 2). It is likely, however, that both of the remaining mechanisms (fluctuations in ambient velocity, fluctuations in the wake) contribute to variation in drag, and evidence to this effect can be gleaned from the data.

To evaluate the role played by turbulent fluctuations in ambient velocity, I rely on indirect evidence based on u^* (a time-averaged index of turbulence) and the similarity between the flow in these experiments and that in a classic set of measurements conducted by Reichardt (1938) and discussed by Schlichting (1979). In a turbulent boundary layer with u^* equal to 5% of the mainstream velocity, Reichardt found that the root mean square velocity deviation u'_{rms} was largest very near the substratum (at 0.07δ , just above the viscous sublayer) and equal to $2.6u^*$. u'_{rms} decreased farther from the wall until, at the top of the boundary layer, $u'_{rms} \approx u^*$ (Fig. 6). Averaged over the boundary layer, $u'_{rms} = 1.19u^*$. I assume that the relationship between u'_{rms} and u^* found by Reichardt (1938) is similar to that in the boundary layer present during these experiments. Comparable results have been obtained in other studies (e.g. Laufer, 1950; Pai, 1953).

Given this assumed similarity and using the friction velocity measured during these experiments (6.6% of u_∞), the average fluctuations in velocity in the experiments performed here are expected to reach a maximum of $2.6 \times 6.6\% = 17.2\%$ of u_∞ very near the wall. For an object with all its exposed area centered at the top of the viscous sublayer, this would result in an average fluctuation in drag of 37.4% of the mean [drag is proportional to the square of velocity (equation 1) and $1.172^2 = 1.374$]. An object whose

area was spread uniformly across the boundary layer (such as a cylinder or rectangular plate) would experience an average fluctuation in velocity of $1.19 \times 6.6\% = 7.9\%$ and an average fluctuation in drag of 16.3%. Objects extending above the boundary layer would experience smaller fluctuations in velocity (averaged across their exposed area) and smaller fluctuations in drag. Note that the estimates made here are for *average* fluctuations in drag; maximal fluctuations will be larger by an amount that cannot be specified without precise knowledge of the frequency and spatial characteristics of extreme velocity deviations.

Several aspects of the data presented here are indeed in accordance with these expectations. First, the sphere (2.17 cm in diameter) and limpet (1.43 cm high) do not extend much beyond the boundary layer (which is approximately 1.2 cm thick) and their modal maximal drags (16% and 18% greater than the mean, respectively, Table 1) fall near the value for the average deviation in drag predicted above (16.3% for an object just spanning the boundary layer).

Note, however, that this is a comparison between a *mean* and a *maximum*. Because the maximal deviation must be larger than the average, any meaningful similarity between the measured maximal and predicted mean forces depends on the response characteristics of the drag transducer. Recall that the most energetic fluctuations in mainstream velocity (those that would lead to the maximal drag) are likely to be applied for a period of approximately 0.01 s, unfortunately too short a time to be measured accurately by the transducer used here (response time 0.024 s). As a consequence, it is possible that the maximal applied drags are attenuated by the transducer just enough to be similar to the mean values predicted. Without fuller knowledge of the frequency spectrum of applied drags, it is impossible to evaluate this critically, however, and it is quite possible that the similarity between measured maximal and predicted mean values for the sphere and limpet is merely coincidental.

Further evidence for the role of ambient velocity fluctuations is found in the fact that the tallest objects used in these experiments (the large cylinder, 4.04 cm high, and the flat plate, 3.03 cm high) show the smallest variation in drag (ϵ , Table 1), as would be expected from the spatial gradient in u'_{rms} shown in Fig. 6. In addition, the small cylinder has a higher modal maximal normalized drag than the large cylinder (8.2% *versus* 6.0% greater than the mean).

Note, however, that the modal maximal Fn of the small cylinder (although higher than that of the large cylinder) is much smaller than that of the sphere (8.2% *versus* 16.1%), which has virtually the same height (small cylinder, 2.25 cm; sphere 2.17 cm). This disparity between objects of the same height suggests that the shape of the object (as well as its size) plays a role in determining the magnitude of drag fluctuations.

In summary, the results obtained here are consistent with the hypothesis that variation in drag in turbulent flow is caused by a combination of two mechanisms: (1) fluctuations in ambient velocity as turbulent eddies are convected past an object (a mechanism for which the size of the object relative to the boundary layer thickness is important) and (2) fluctuations in wake pressure as eddies are shed (a mechanism in which the shape of the object is important). Further investigation of these mechanisms will require direct,

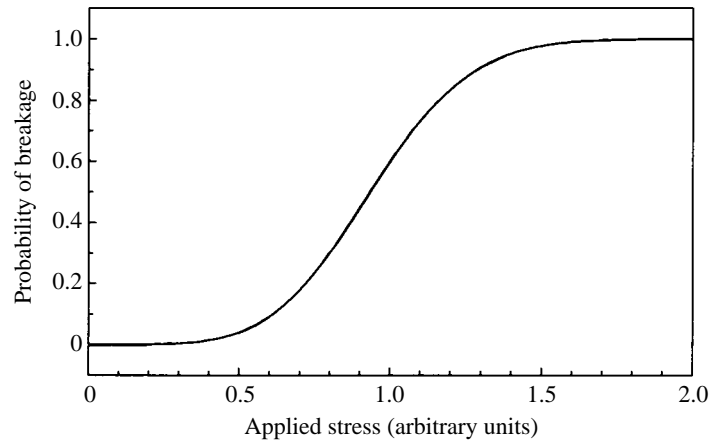


Fig. 7. A hypothetical cumulative curve of the probability that an organism (chosen at random) has less than a specified strength.

simultaneous measurements of both the local fluctuations in ambient and wake velocities and the instantaneous drag imposed on an object.

Biological consequences

Of what biological importance is the variation in drag measured here? The most obvious consequence concerns the likelihood that an organism will be dislodged or broken: the larger the drag, the greater the probability of breakage. But the relationship between an increase in drag and the consequent increase in breakage is not necessarily linear. That is, a 10% increase in drag could, under certain circumstances, lead to only a 2% increase in breakage while under other circumstances leading to a 50% increase. This nonlinearity complicates the interpretation of the effects of drag, and is briefly explored here.

When drag is imposed on an organism, stress is placed on its structure. If the imposed stress exceeds the strength of the most susceptible element of the structure, the organism is broken or dislodged. Until a structure is actually broken, however, its strength can only be described in a probabilistic fashion (Alexander, 1981; Denny, 1988). The chance nature of breakage can be conveniently quantified as a graph of the cumulative probability of breakage as a function of applied stress; a typical example is shown in Fig. 7. Below a certain applied stress (in this hypothetical case, about 0.3 arbitrary units), the probability of breakage is very low and an increase in applied stress results in a negligible increase in the risk of breakage. The same is true for very large applied stresses: if a given stress results in a 99% probability of breakage, increasing the applied stress cannot lead to any substantial increase in risk. Stated in another way, at very low or very high applied stresses, the slope of the cumulative probability curve is small.

Near the median breaking stress (the stress that results in a 0.5 probability of breakage), the slope of the curve is greatest and the increase in probability of breakage associated with an increase in applied stress is maximal. In this region, the slope of the curve is very sensitive to the variation in strength found in the population; the less variable the strength

(the smaller its standard deviation), the less the ‘spread’ in the cumulative probability, and the steeper is the curve. Given a small standard deviation, a small increase in stress near the median can result in a large increase in risk.

It is apparent, then, that the increase in the risk of breakage associated with the maximal (as opposed to the mean) drag depends on three factors: (1) the fractional increase in drag, (2) the location of the mean applied stress on the cumulative probability curve, and (3) the standard deviation of the strength distribution.

Let us assume that we have measured the strengths exhibited by a given population of organisms and can express the stress required to break each organism as a fraction, S , of the mean breaking stress of the population. Here, I assume that the distribution of S is Gaussian, a simplifying assumption based on evidence from a variety of intertidal algae and invertebrates (Gaylord *et al.* 1994; M. W. Denny, unpublished data). Given this assumption, the probability that an organism chosen at random from the population has a strength less than or equal to S is:

$$P(S) = \int_0^S \frac{1}{\sigma\sqrt{2\pi}} \exp \left\{ - \left[\frac{(x-1)^2}{2\sigma^2} \right] dx \right\}, \quad (11)$$

where σ is the standard deviation of the distribution (Zar, 1974). Note that, because we have normalized stress to the population mean, the mean normalized stress is equal to 1 and the coefficient of variation (CV, σ divided by the mean) is therefore equal to the standard deviation.

The organism is now exposed to flow that is characterized by a mean velocity and rapid turbulent fluctuations about this mean. In nature, the mean velocity itself may vary through time (a complication discussed below), but we assume that the variation in the mean is very slow compared with the high-frequency fluctuations due to turbulence, allowing us to calculate a reasonable mean velocity for a given period. This mean velocity results in a mean drag which, in turn, places a normalized stress, S_{mean} , on the organism’s structure. The maximal drag, however, imposes a larger stress, S_{max} , which (unlike S_{mean} within the period of measurement) is a function of time (see equation 10). The difference in probability of dislodgment between that due to the maximal and mean drags, R :

$$R = P(S_{\text{max}}) - P(S_{\text{mean}}), \quad (12)$$

is the increase in the predicted risk of dislodgment or breakage associated with the observed fluctuation in drag for the given period. The magnitude of R depends on S_{mean} , on S_{max} (and thus time) and on the distribution of S , indexed by its coefficient of variation.

In a 1 h exposure to turbulent flow with a constant mean, the limpet examined in this study has an expected maximal drag that exceeds the mean by 33 % (equation 10), a value we use as a heuristic example. The increase in risk, R , associated with the imposition of this maximal force (rather than the mean force) is:

$$R = P(1.33S_{\text{mean}}) - P(S_{\text{mean}}), \quad (13)$$

shown in Fig. 8 as a function of S_{mean} for a range of coefficients of variation. As noted above, the *increase* in risk of breakage or dislodgment is relatively small unless the stress

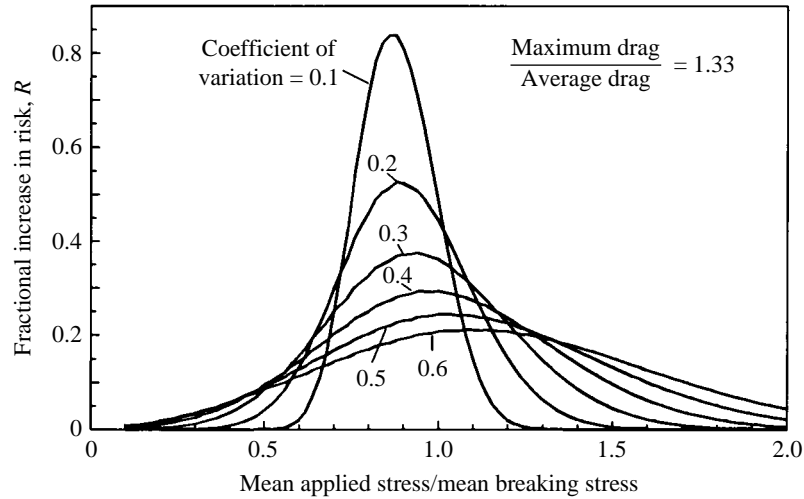


Fig. 8. The imposition of a maximal drag results in an increase in the risk of dislodgment R above that predicted for the imposition of the mean drag. The magnitude of this increase is shown as a function of the ratio of mean drag-imposed stress to the population mean breaking stress, S_{mean} .

applied by the mean drag is near the mean (=median) strength of the population ($S=1$). For S_{mean} less than about 0.4 or greater than 1.8, there is little increase in risk caused by a 33% increase in drag.

In contrast, when the stress applied by the mean drag is near the mean strength (S_{mean} is near 1), the additional risk associated with fluctuations in drag can be quite high. For example, the maximal increase in risk associated with a 33% increase in drag is approximately 80% if the coefficient of variation is 0.1 (Fig. 8). This amplification of the effect of increased drag depends, however, on the coefficient of variation. For S_{mean}

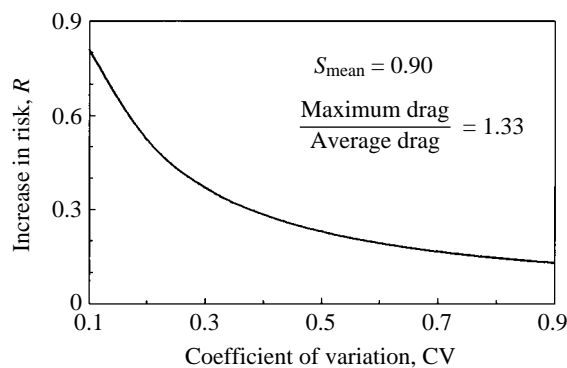


Fig. 9. Increase in risk, R , as a function of the coefficient of variation of strength for $S_{\text{mean}}=0.90$ and $S_{\text{max}}/S_{\text{mean}}=1.33$. For small coefficients of variation, the increase in risk is large relative to the increase in drag.

values near 1, the larger the CV, the smaller the increase in risk associated with an increase in drag (Fig. 9).

Where on Fig. 8 has nature placed real benthic organisms? It is likely that most sessile organisms are sufficiently well adapted to their surroundings that they face little day-to-day risk of breakage from fluid-dynamic forces (Vogel, 1981; Denny, 1988). In these cases ($S_{\text{mean}} < 0.5$), the increase in risk due to fluctuations in drag is likely to be small.

Under certain conditions, however, stationary organisms may be placed under fluid-imposed stresses that fall near the population's mean strength (on the steep portion of their cumulative probability curves), and the effects of any increase in drag could be amplified. For example, Tunnicliffe (1981) found that 80% of a population of staghorn coral (*Acropora cervicornis*) had broken at their base, equivalent to an S_{max} of 1.21 if the strength of these corals is normally distributed. Data presented by Putz and Milton (1982) and Putz *et al.* (1983) suggest that, in a lifetime of 50–100 years, a tree in a tropical forest has a 34–54% chance of uprooting or snapping; damage caused, at least in part, by wind loading. These probabilities are equivalent to an S_{max} of 0.85–1.04. Paine and Levin (1981) report that as many as 41–63% of the mussels (*Mytilus californianus*) present on a shore can be dislodged in a single winter, equivalent to an S_{max} of 0.93–1.11. In these cases, S_{mean} (which will be somewhat less than S_{max}) may fall near 1, and it is possible that any increase in maximal drag would result in an amplified response in the probability of breakage.

The coefficients of variation for these species are large, however. The CV for *A. cervicornis* is 0.25 (Denny, 1988), for the trees examined by Putz and Milton (1982) the CV of wood strength was 0.38 (Putz *et al.* 1983), and for mussels at the site used by Paine and Levin (1981), the CV of attachment strength was 0.32 (Denny *et al.* 1985). In all of these cases, CV values are large enough to reduce or negate the amplification of risk due to increased drag: a 33% increase in drag would result in a maximal 35–50% increase in risk of breakage. It is conceivable that these organisms have 'hedged their bets' in terms of drag-induced breakage by presenting to the environment a wide range of strengths.

It should be noted that there is likely to be a cost associated with the production by an individual coral, tree or mussel of progeny with a large CV of strength. The wider their spread in strength, the larger the fraction of these offspring that is poorly designed to resist drag. The very weak individuals are likely to be broken before they reproduce and the very strong individuals may have a lower reproductive output because of the additional material and energy expended in becoming overly strong.

A scenario can thus be envisioned in which an optimal CV exists for the persistence of a given species in a given environment. Too small a CV means that chance variation in applied stress (such as that documented here for drag) will result in a greatly amplified risk of breakage. Too large a CV entails the cost associated with misallocation of resources in unnecessarily strong individuals.

Unfortunately, sufficient data do not exist for a critical examination of this proposition. Coefficients of variation in strength have been measured for only a few sessile organisms, and these are highly variable. For example, the CVs reported for corals range from 0.25 to 0.73 (Chamberlain, 1978; Vosburgh, 1982; Denny *et al.* 1985; Denny, 1988). The

adhesive strengths of limpets have CVs that vary between 0.15 and 0.93 (Branch and Marsh, 1978; Grenon and Walker, 1981; Denny *et al.* 1985; Denny, 1989; Hahn and Denny, 1989). Snails exhibit adhesive strengths with CVs that vary from 0.19 to 0.66 (Miller, 1974), and the strengths of various benthic algae have CVs that vary from 0.22 to 0.88 (Koehl and Wainwright, 1977; Denny *et al.* 1989; Kraemer and Chapman 1991). Barnacles have a smaller range, 0.3–0.53 (Yule and Walker, 1984; Denny *et al.* 1985), but this may simply be due to the smaller number of species on which measurements have been conducted.

In summary, the effects of drag fluctuations on survival depend on the magnitude of the mean imposed stress relative to the mean strength, on the ratio of maximal to mean drag (a function of time) and on the coefficient of variation of strength. All of these values vary in nature, but cases exist in which drag fluctuations are likely to result in a substantial increase in the risk of breakage or dislodgment.

Variability in drag of the type described here may also have important effects on the evolution of safety factors in organisms susceptible to dislodgment by this fluid-dynamic force. Here, safety factor is defined as the ratio of the predicted strength of an organism (that is, the mean strength of the population) to the predicted maximal force that the organism will experience. Alexander (1981) and Lowell (1985, 1987) note that increased environmental variability (of which drag may be an important component) is expected to result in the evolution of an increased safety factor, and Lowell (1987) presents evidence that safety factors can indeed evolve in response to the environment. In the present context, one would expect that the observed fluctuations in drag may set a lower limit to the appropriate safety factor for stationary organisms exposed to flow. Shapes or sizes of organisms that have a relatively large maximal drag (such as the limpet tested here) should have relatively large safety factors in the structures affected by drag.

Note that the calculations leading to Figs 8 and 9 assume a Gaussian distribution of strengths. A non-normal distribution would lead to quantitatively different results, but the deviation from normality would have to be large to change the results qualitatively.

Note also that the hypothetical examples cited here have assumed an increase in drag of 33% above the mean, a value appropriate for a limpet exposed to flow for 1 h. Longer exposures would lead to more extreme drags (Fig. 5) and larger increases in risk than those discussed here.

Variations in mean velocity

The turbulence-induced increases in drag discussed here have been measured relative to a mean drag that, for simplicity, has been assumed to be constant. In nature, the mean velocity in a turbulent flow (and hence the mean drag) is very likely to change through time. In times of flood, the mean velocity in a stream or river will be higher than in times of drought; the mean wind velocity will be higher in storms than on calm days. The flow beneath ocean waves is an extreme case. On a wave-swept shore, the bulk velocity of water oscillates with a typical period of 4–10 s, and the separation of a mean velocity from the turbulence-induced fluctuations can be problematic. In many of these cases, the variation in drag due to variation in the mean velocity may be larger than the variation due to turbulence.

It is important to note, however, that the two sources of variation are additive. During a

period when mean drag is high, the maximal drag on an object will be higher still due to the effects of turbulence explored here. Regardless of any variation in mean velocity, the accurate prediction of maximal drag requires that attention be paid to the effects of turbulence.

For a discussion of a method by which the maximal mean velocity can be predicted for a given environment, see Denny (1988, 1991, 1993, 1994) and Gaines and Denny (1993).

Caveats

It must be stressed that the probabilities of observing a given maximal drag presented here apply only to the particular flow conditions of these measurements, to the particular objects used in these experiments and to the particular compliance of the transducer. It remains to be seen whether the results for these specific objects can be generalized to different velocities and different intensities of turbulence, and it may be that other objects will show different variation in their extreme drags even under conditions identical to those used here. Furthermore, as discussed above, very rigid objects in nature are likely to experience more extreme forces than those recorded here, just as objects mounted on a more rigid force transducer would. In this respect, it would be advantageous to repeat the experiments conducted here using a variety of live organisms mounted on a very stiff force transducer. In this fashion, the compliance of the organism itself (rather than that of the transducer) would control the 'filtering' of turbulence-induced forces.

This report describes forces in steady unidirectional flow, and care must be taken if these results are to be extrapolated to other situations. For example, if the mean flow velocity varies slowly through time (owing to factors other than turbulence), the period used to calculate the mean velocity may affect the results. If the period chosen is too long, several fluctuations in the mean may be included, and these fluctuations may appear, to the present method of analysis, as an increase in the turbulence-induced deviations in force. It was to avoid the possibility of this error that the maximal drags measured in these experiments were compared with an electronically filtered instantaneous mean (essentially a running mean of forces within 1 s of the time when the maximum was measured) rather than with the mean drag for the entire measurement period. Special care should be exercised if the results described here are to be applied to cases where the direction (as well as the velocity) of mainstream flow varies through time. For example, it is unclear what effect the wake of an object will have when, after a shift in the direction of flow, it is carried back past its origin.

As a further complication, drag is only one of several hydrodynamic forces acting on benthic organisms. Lift, like drag, results from the pressure distribution around an organism (Vogel, 1981; Denny, 1988, 1989) and may perhaps show a similar pattern of extremes in turbulent flow (Willems and Murray, 1981). The behavior of accelerational forces is much more complicated than that of drag or lift (Denny *et al.* 1985; Denny, 1988; Gaylord *et al.* 1994), and it is premature even to speculate on how these forces interact with turbulence. Until we have a better understanding of each of these forces separately and of their interaction under field conditions, the prediction of the biological effects of hydrodynamic forces will remain an inexact science.

In conclusion, the maximal drag imposed on a stationary organism in turbulent flow

exceeds the mean drag by an amount that depends both on the shape and size of the object and on the time for which the object is subjected to flow. For example, the maximal drag imposed on a sphere under the conditions used in these experiments is likely to be 16% greater than the mean in an exposure of only 20 s and may reach values greater than three times the mean during lengthy exposures. The extreme drags imposed in turbulent flow can result in substantially greater dislodgment and breakage of stationary organisms than would be predicted from the mean drag. It would therefore be dangerous to predict the biological consequences of fluid-dynamic forces without taking into account the stochastic variation of these forces in turbulent flow.

The magnitude of drag variation for a given organism is likely to depend on the intensity of turbulence, the size of the organism relative to the boundary-layer thickness and the shape of the organism. Further research is required, however, to explore the precise mechanism(s) that cause the observed variation in drag and to extend the observations made here to a wider variety of flows.

I thank B. Gaylord, E. C. Bell, K. Mead, C. A. Butman, B. Hale and two anonymous reviewers for helpful comments on the manuscript. This work was supported by NSF Grant OCE-9115688.

References

- ALEXANDER, R. MCN. (1981). Factors of safety in the structure of animals. *Scient. Prog.* **67**, 109–130.
- BRANCH, G. M. AND MARSH, C. (1978). Tenacity and shell shape in six *Patella* species: adaptive features. *J. exp. mar. Biol. Ecol.* **34**, 111–130.
- CANTWELL, B. J. (1981). Organized motion in turbulent flow. *A. Rev. Fluid Mech.* **13**, 457–515.
- CARRINGTON, E. (1990). Drag and dislodgment of an intertidal macroalga: consequences of morphological variation in *Mastocarpus papillatus* Kützing. *J. exp. mar. Biol. Ecol.* **139**, 185–200.
- CHAMBERLAIN, J. A. (1978). Mechanical properties of coral skeleton: compressive strength and its adaptive significance. *Paleobiology* **4**, 419–435.
- DENNY, M. W. (1988). *Biology and the Mechanics of the Wave-Swept Environment*. Princeton, NJ: Princeton University Press.
- DENNY, M. W. (1989). A limpet shell that reduces drag: laboratory demonstration of a hydrodynamic mechanism and an exploration of its effectiveness in nature. *Can. J. Zool.* **67**, 2098–2106.
- DENNY, M. W. (1991). Biology, natural selection and the prediction of maximal wave-induced forces. *S. Afr. J. mar. Sci.* **10**, 353–363.
- DENNY, M. W. (1993). Disturbance, natural selection and the prediction of maximal wave-induced forces. *Contemp. Math.* **141**, 65–81.
- DENNY, M. W. (1994). Roles of hydrodynamics in the study of life on wave-swept shores. In *Ecomorphology*, chapter 8 (ed. P. C. Wainwright and S. Reilly). Chicago: University of Chicago Press.
- DENNY, M. W., BROWN, V., CARRINGTON, E., KAEMER, G. AND MILLER, A. (1989). Fracture mechanics and the survival of wave-swept macroalgae. *J. exp. mar. Biol. Ecol.* **127**, 211–228.
- DENNY, M. W., DANIEL, T. L. AND KOEHL, M. A. R. (1985). Mechanical limits to size in wave-swept organisms. *Ecol. Monogr.* **55**, 69–102.
- DENNY, M. W. AND GAINES, S. (1990). On the prediction of maximal intertidal wave forces. *Limnol. Oceanogr.* **35**, 1–15.
- EFRON, B. AND TIBSHIRANI, R. (1993). *An Introduction to the Bootstrap*. New York: Chapman and Hall.
- GAINES, S. AND DENNY, M. W. (1993). The largest, smallest, highest, lowest, longest and shortest: extremes in ecology. *Ecology* **74**, 1677–1692.
- GAYLORD, B., BLANCHETTE, C. AND DENNY, M. (1994). Mechanical consequences of size in wave-swept macroalgae. *Ecol. Monogr.* (in press).

- GRACE, J. (1977). *Plant Response to Wind*. London: Academic Press.
- GRENON, J.-F. AND WALKER, G. (1981). The tenacity of the limpet, *Patella vulgata* L.: an experimental approach. *J. exp. mar. Biol. Ecol.* **54**, 277–308.
- GUMBEL, E. J. (1958). *Statistics of Extremes*. New York: Columbia University Press.
- HAHN, T. AND DENNY, M. (1989). Tenacity-mediated selective predation by oystercatchers on intertidal limpets and its role in maintaining habitat partitioning by '*Collisella*' *scabra* and *Lottia digitalis*. *Mar. Ecol. Progr. Ser.* **53**, 1–10.
- HYNES, H. B. N. (1970). *The Ecology of Running Waters*. Toronto: University of Toronto Press.
- JACOBS, J. L. AND KNEILE, K. R. (1975). Statistical prediction of maximum time-variant inlet distortion levels. *Arnold Eng. Develop. Center Tech. Rep.* AD/A-004 104.
- KOEHL, M. A. R. (1984). How do benthic organisms withstand moving water? *Am. Zool.* **24**, 57–70.
- KOEHL, M. A. R. AND WAINWRIGHT, S. A. (1977). Mechanical adaptations of a giant kelp. *Limnol. Oceanogr.* **22**, 1067–1071.
- KRAEMER, G. P. AND CHAPMAN, D. J. (1991). Biomechanics and alginic acid composition during hydrodynamic adaptation by *Egregia menziesii* (Phaeophyta) juveniles. *J. Phycol.* **27**, 47–53.
- LAUFER, J. (1950). Some recent measurements in a two-dimensional turbulent channel. *J. aeronaut. Sci.* **17**, 277–287.
- LOWELL, R. B. (1985). Selection for increased safety factors of biological structures as environmental unpredictability increases. *Science* **228**, 1009–1011.
- LOWELL, R. B. (1987). Safety factors of tropical versus temperate limpet shells: multiple selection pressures on a single structure. *Evolution* **41**, 638–650.
- MIDDLETON, G. V. AND SOUTHWARD, J. B. (1984). *Mechanics of Sediment Movement*. Tulsa, Oklahoma: Society of Economic Paleontologists and Mineralogists.
- MILLER, S. L. (1974). Adaptive design of locomotion and foot form in prosobranch gastropods. *J. exp. mar. Biol. Ecol.* **14**, 99–156.
- OLIVER, H. R. AND MAYHEAD, G. J. (1974). Wind measurements in a pine forest during a destructive gale. *Forestry* **47**, 185–194.
- PAI, S. I. (1953). On turbulent flow between parallel plates. *J. appl. Mech.* **20**, 109–114.
- PAINE, R. T. AND LEVIN, S. (1981). Intertidal landscapes: disturbance and the dynamics of pattern. *Ecol. Monogr.* **51**, 145–178.
- PUTZ, F. E., COLEY, P. D., LU, K., MONTALVO, A. AND AIELLO, A. (1983). Uprooting and snapping of trees: structural determinants and ecological consequences. *Can. J. For. Res.* **13**, 1011–1020.
- PUTZ, F. E. AND MILTON, K. (1982). Tree mortality rates on Barro Colorado Island, Panama. In *The Ecology of a Tropical Rain Forest: Seasonal Rhythms and Longer-Term Changes* (ed. E. G. Leigh, Jr, D. M. Windsor and A. S. Rand). Washington, DC: Smithsonian Institution Press.
- REICHARDT, H. (1938). Messungen turbulenter Schwankungen. *Naturwissenschaften* **26**, 404–408.
- SARPKAYA, T. AND ISAACSON, M. ST. Q. (1981). *Mechanics of Wave Forces on Offshore Structures*. New York: Van Nostrand Reinhold.
- SCHLICHTING, H. (1979). *Boundary-Layer Theory*. 7th edn. New York: MacGraw Hill.
- SEYMOUR, R. J., TEGNER, M. J., DAYTON, P. K. AND PARNELL, P. E. (1989). Storm wave induced mortality of the giant kelp, *Macrocystis pyrifera*, in southern California. *Estuar. coastal Shelf Sci.* **28**, 277–292.
- TENNEKES, H. AND LUMLEY, J. L. (1972). *A First Course in Turbulence*. Cambridge, MA: MIT Press.
- TUNNICLIFFE, V. (1981). Breakage and propagation of the stony coral *Acropora cervicornis*. *Proc. natn. Acad. Sci. U.S.A.* **78**, 2427–2431.
- VOGEL, S. (1981). *Life in Moving Fluids*. Princeton, NJ: Princeton University Press.
- VOSBURGH, F. (1982). *Acropora reticulata*: structure, mechanics and ecology of a reef coral. *Proc. R. Soc. Lond.* **214**, 481–499.
- WILLIAMS, J. J., THORNE, P. D. AND HEATHERSHAW, A. D. (1989). Measurement of turbulence in the benthic boundary layer over a gravel bed. *Sedimentology* **36**, 959–971.
- WILLETTS, B. B. AND MURRAY, C. G. (1981). Lift exerted on stationary spheres in turbulent flow. *J. Fluid Mech.* **105**, 487–505.
- YULE, A. B. AND WALKER, G. (1984). The adhesion of the barnacle, *Balanus balanoides*, to slate surfaces. *J. mar. biol. Ass. U.K.* **64**, 147–156.
- ZAR, J. H. (1974). *Biostatistical Analysis*. Englewood Cliffs, NJ: Prentice-Hall.